



Available online at <http://scik.org>

Commun. Math. Biol. Neurosci. 2023, 2023:96

<https://doi.org/10.28919/cmbn/8161>

ISSN: 2052-2541

## SENSITIVITY ANALYSIS AND OPTIMAL COUNTERMEASURES CONTROL OF MODEL OF THE SPREAD OF COVID-19 CO-INFECTION WITH HIV/AIDS

JONNER NAINGGOLAN<sup>1,\*</sup>, JOKO HARIANTO<sup>1</sup>, MOCH. FANDI ANSORI<sup>2</sup>

<sup>1</sup>Department of Mathematics, Faculty of Mathematics and Natural Sciences, Universitas Cenderawasih, Jayapura, 99224, Indonesia

<sup>2</sup>Department of Mathematics, Faculty of Science and Mathematics, Universitas Diponegoro, Semarang, 50275, Indonesia

Copyright © 2023 the author(s). This is an open access article distributed under the Creative Commons Attribution License, which permits unrestricted use, distribution, and reproduction in any medium, provided the original work is properly cited.

**Abstract:** This paper analyzes and examines the optimal control in the co-infection of COVID-19 with HIV/AIDS by providing preventive and treatment control measures. The population is divided into eight subpopulations. The preventive control of COVID-19 is denoted by  $u_1$ . The preventive control of HIV/AIDS is denoted by  $u_2$ . The treatment control of COVID-19 is denoted by  $u_3$ , and the treatment control of COVID-19 for the subpopulation co-infected with HIV/AIDS is denoted by  $u_4$ . Based on the model analysis, non-endemic and endemic equilibrium points are obtained, along with the basic reproduction number of the COVID-19, HIV/AIDS, and COVID-19-HIV/AIDS sub-models. Numerical simulations reveal that using preventive control  $u_1$  is more effective in reducing the spread of COVID-19 compared to  $u_3$  or  $u_4$ , both individually and together. Preventive control  $u_2$  is more effective in controlling the spread of HIV/AIDS compared to the absence of control. The sensitivity analysis of parameter identifies parameters that significantly affect the reduction or increase in the spread of COVID-19-HIV/AIDS co-infection. We found that in order to reduce the co-infection's spread, we should pay attention to the reducing the contact rate of HIV/AIDS patients

---

\*Corresponding author

E-mail address: [jonner2766@gmail.com](mailto:jonner2766@gmail.com)

Received August 4, 2023

or increasing their treatment rate.

**Keywords:** COVID-HIV/AIDS co-infection; equilibrium points; the basic reproduction number; sensitivity analysis; optimal control.

**2020 AMS Subject Classification:** 92D25, 93A30.

## 1. INTRODUCTION

The COVID-19 disease has subsided since the end of 2022, but it has had a significantly adverse impact on health, economy, education, social and cultural progress [1]. The pattern of COVID-19 transmission with HIV/AIDS differs, but individuals with HIV may experience a higher prevalence of infection and COVID-19 complications compared to those without HIV [2]. Co-infection of COVID-19 with congenital diseases has led to numerous fatalities, including comorbidities with HIV/AIDS. Mathematics plays a pivotal role in modeling, analyzing, predicting, controlling, and optimizing the spread of infectious diseases [1].

The mathematical model of the COVID-19 disease spread in Wuhan was studied and analyzed in 2020 [3]. Ahmed (2021) conducted an analysis of the disease spread in the country, considering both symptomatic and asymptomatic cases [4]. The majority of COVID-19 fatalities were attributed to individuals with underlying congenital diseases [1]. A study examining COVID-19 in the context of hereditary diseases was conducted to identify relevant parameters for disease control [5]. In order to optimize the control of COVID-19, preventive measures, isolation, and treatment strategies are implemented [6]. The spread of HIV/AIDS can occur through needles and sexual relations [2], [7]. Massarvva (2021) conducted a literature review on addressing COVID-19 and HIV co-infection based on previous study findings [8]. It is essential to analyze optimal controls to reduce and prevent the spread of HIV, considering non-endemic, endemic, and threshold stability [9].

HIV-infected individuals who contract malaria are at risk of experiencing an increase in HIV virus levels in their bodies, thereby amplifying the chances of HIV transmission to their partners [10], [11]. The transmission pattern of malaria co-infection with HIV/AIDS is nearly identical to that of dengue fever co-infection with HIV/AIDS [12]. The diseases co-infected with HIV, such as

tuberculosis, can be studied to analyze the necessary parameters for optimizing the control of such co-infections [13], as well as co-infection studies with Human T-cell leukemia virus (HTLV) [14]. COVID-19 infection can worsen if infected individuals are not screened for congenital diseases [15]. The rise in mortality due to COVID-19 infection necessitates investigations into comorbid diseases with SARS [16].

The moderate increase in the risk of death is directly related to COVID-19 infection, with findings indicating that the risk of death for patients with HIV-positive comorbidities is almost double compared to patients with HIV-negative comorbidities [2]. The effects of tuberculosis and HIV-1 infection on the dynamics of COVID-19 spread and immune response were investigated, particularly in Africa [13], [17]. Elaiw (2022) conducted a global analysis of the HIV and SARS co-infection model, observing the interaction between healthy and latency epithelial cells [16]. HIV-infected patients have a higher likelihood of being infected with COVID-19, and the consequences of HIV disease are independently and positively correlated with increased mortality in patients with COVID-19 [18]. The role of digital health and HIV and COVID-19 care management has an impact on the cure rate for HIV, COVID, and co-infection of the two diseases [19]. People with HIV have a similar risk of severe COVID-19 infection compared to the general population [20], [21]. The COVID-19/AIDS co-infection model was employed to observe the effect on uninfected epithelial cells, infected epithelial cells, and free HIV-1 particles, aiming to reduce viral load in the host [22]. Teklu (2023) conducted numerical simulations in the study of the COVID-19/HIV model to identify the parameters that need intervention to decrease the number of infected individuals [23]. An evaluation of the effect of COVID-19-HIV-TB co-infection on decreasing people's income was conducted using a combination of protocols and the Burkina Faso method [24].

To optimize the reduction of the spread of COVID-19 or HIV, the government is making efforts to provide prevention and treatment controls [1], [2]. Implementing controls to optimally manage COVID-19/HIV co-infection can effectively prevent the spread of both COVID-19 and HIV [25]. A study conducted in southern Africa demonstrated that prevention and care interventions for individuals infected with HIV and COVID-19 had an impact on the severity of COVID-19

infection [26]. Numerical simulations yielded results on the problem of optimal control, suggesting the most effective combination of prevention and treatment strategies to minimize the transmission of HIV/AIDS and COVID-19 co-infection in the community. Building upon the model developed by Teklu et al. (2023) [23], the author focused on vaccination parameters and subsequently examined the optimal prevention control for HIV/AIDS, as well as the optimal prevention and treatment control for COVID-19.

## 2. MODEL FORMULATION AND ANALYSIS

The population is categorized into eight subpopulations as follows: Susceptible subpopulation ( $S$ ): This group comprises individuals who are still healthy but susceptible to infection with COVID-19 or HIV/AIDS. Vaccination subpopulation ( $V_C$ ): This group consists of individuals who are healthy and have been vaccinated against COVID-19. HIV/AIDS protected subpopulation ( $P_H$ ): Individuals in this group have received cellular immune antibody vaccines against the HIV virus, providing protection. Subpopulation infected with COVID-19 ( $I_C$ ): This subpopulation includes individuals who have already been infected with COVID-19. HIV/AIDS-infected subpopulation ( $I_H$ ): Individuals in this subpopulation are already infected with HIV/AIDS. Subpopulations co-infected with COVID-19 and HIV/AIDS ( $C$ ): This group comprises individuals who are simultaneously infected with both COVID-19 and HIV/AIDS. Treatment subpopulation ( $T_H$ ): This group includes individuals infected with HIV/AIDS who are undergoing treatment. Recovered subpopulation ( $R$ ): Individuals in this category are either immune to or have recovered from COVID-19 or are protected against HIV/AIDS.

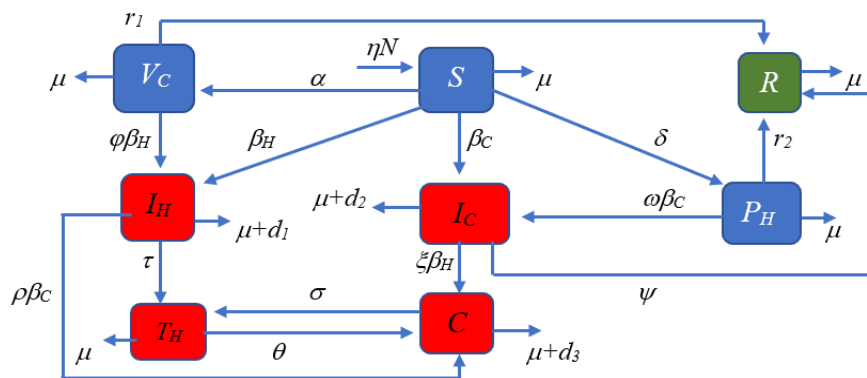


Figure 1. The dynamics of the spread of COVID-19 co-infection with HIV/AIDS

Table 1. Parameter values for low transmission cases of COVID-19 co-infection with HIV/AIDS

Parameter	Description	Value	Referensi
$\Lambda$	Recruitment rate into the subpopulation $S$	2500	[26]
$\alpha$	Vaccination rates from subpopulation $S$ to $V_C$	0.0015	[26]
$\delta$	Vaccination rates from subpopulation $S$ to $P_H$	0.0004	[26]
$\beta_1$	S subpopulation contact rate with $I_C$ and $C$	0.1175	[26]
$\gamma_1$	S subpopulation contact rate with $\beta_1 C$	0.1	[23]
$\beta_2$	S subpopulation contact rate with $I_H$ and $C$	0.3425	[26]
$\gamma_2$	S subpopulation contact rate with $\beta_2 C$	0.12	[23]
$\mu$	The natural death rate of each compartment	$\frac{1}{65 \times 365}$	[26]
$r_1$	Rate of recovered from $V_C$ subpopulation to $R$	0.036]	[26]
$\varphi$	Transfer rate of the $V_C$ subpopulation to $I_H$	0.081	[26]
$r_2$	Recovered rate of $P_H$ subpopulation to $R$	0.0667	[26]
$\omega$	Transfer rate of $P_H$ subpopulations to $I_C$	0.081	[26]
$\psi$	Cure rates of the $I_C$ subpopulation	0.005	[26]
$\xi$	Co-infection rates of the $I_C$ subpopulation to $C$	0.1	[23]
$d_1$	Mortality rate in the $I_H$ subpopulation	0.00023	[23]
$d_2$	Mortality rate in the $I_C$ subpopulation	0.15	[26]
$\tau$	Treatment rates in the $I_H$ subpopulation	0.024	assumed
$\rho$	$I_H$ subpopulation infection rate to $C$	0.12	[23]
$\theta$	$T_H$ subpopulation infection rate to $C$	0.11	assumed
$\sigma$	The cure rate of the subpopulation $C$ from COVID-19	0.005	[23]
$d_3$	Mortality rate in subpopulation $C$	0.15	[26]

The assumptions of the model studied in this research are as follows: (1) The recruitment rate into the susceptible subpopulation takes into account COVID-19 vaccination and cellular immune

antibody against the HIV virus. (2) Vaccinated individuals have a possibility of immunity against COVID-19 or HIV/AIDS. (3) Individuals infected with COVID-19 and receiving treatment have a chance of recovery. (4) Individuals infected with COVID-19 or HIV/AIDS may potentially experience COVID-19 and HIV/AIDS co-infection. (5) Each subpopulation has a natural mortality rate, and individuals in the  $I_C$ ,  $I_H$ , or  $C$  subpopulations may die due to illness. The schematic diagram of the studied model is shown in Figure 1 below.

The differential equation system of the model of the spread of COVID-19 infection with HIV/AIDS is as follows:

$$\left. \begin{aligned} \frac{dS}{dt} &= \Lambda - (\alpha + \delta + \beta_C + \beta_H + \mu)S \\ \frac{dV_C}{dt} &= \alpha S - (r_1 + \varphi\beta_H + \mu)V_C \\ \frac{dP_H}{dt} &= \delta S - (r_2 + \omega\beta_C + \mu)P_H \\ \frac{dI_C}{dt} &= \beta_C S + \omega\beta_C P_H - (\psi + \xi\beta_H + d_2 + \mu)I_C \\ \frac{dI_H}{dt} &= \beta_H S + \varphi\beta_H V_C - (\tau + \rho\beta_C + d_1 + \mu)I_H \\ \frac{dC}{dt} &= \xi\beta_H I_C + \rho\beta_C I_H + \theta T_H - (\sigma + d_3 + \mu)C \\ \frac{dT_H}{dt} &= \tau I_H + \sigma C - (\theta + \mu)T_H \\ \frac{dR}{dt} &= r_1 V_C + r_2 P_H + \psi I_C - \mu R \end{aligned} \right\} \quad (1)$$

with  $\beta_C(t) = \frac{\beta_1}{N}(I_C(t) + \gamma_1 C(t))$ ,  $\beta_H(t) = \frac{\beta_2}{N}(I_H(t) + \gamma_2 C(t))$ .

Notation of parameters, description, and value of parameters as shown in Table 1.

## 2.1 COVID-19 Sub-Model

This case is only considered for the spread of COVID-19, so in this case,  $P_H = I_H = T_H = C = R = 0$ . Thus, the sub-model for the case of the spread of COVID-19 is given by the following system of differential equations

$$\left. \begin{aligned} \frac{dS}{dt} &= \Lambda - \left( \alpha + \delta + \frac{\beta_1}{N_C} I_C + \mu \right) S \\ \frac{dV_C}{dt} &= \alpha S - (r_1 + \mu) V_C \\ \frac{dI_C}{dt} &= \frac{\beta_1}{N_C} S I_C - (\psi + d_2 + \mu) I_C \end{aligned} \right\} \quad (2)$$

with  $N_C = S + V_C + I_C$ . All equilibrium points of System (2) can be obtained by solving the following system of equations

$$\frac{dS}{dt} = \frac{dV_C}{dt} = \frac{dI_C}{dt} = 0.$$

One of the equilibrium points, which is often referred to as the disease-free equilibrium point ( $E_C^0$ ), is obtained when  $I_C = 0$ . The disease-free equilibrium point for the sub-model of the spread of COVID-19, namely

$$E_C^0 = (S^0, V_C^0, I_C^0) = \left( \frac{\Lambda}{\alpha + \delta + \mu}, \frac{\alpha \Lambda}{(\alpha + \delta + \mu)(r_1 + \mu)}, 0 \right).$$

The basic reproduction number of System (2) is determined using the next-generation matrix [27]. Based on System (2), the  $F$  and  $V$  matrices are obtained as follows:

$$F = \begin{pmatrix} \frac{\beta_1}{N_C^0} S^0 & 0 \\ 0 & 0 \end{pmatrix}, \quad V = \begin{pmatrix} \psi + d_2 + \mu & 0 \\ 0 & r_1 + \mu \end{pmatrix},$$

with  $N_C^0 = S^0 + V_C^0 + I_C^0$ .

so that the next-generation matrix is obtained as follows:

$$FV^{-1} = \begin{pmatrix} \frac{\beta_1(r_1 + \mu)}{(r_1 + \mu + \alpha)(\psi + d_2 + \mu)} & 0 \\ 0 & 0 \end{pmatrix}.$$

The basic reproduction number of System (1) is the maximum eigenvalue of the  $FV^{-1}$  matrix. So, by using the next-generation matrix, it is obtained the basic reproduction number for the sub-model of the spread of COVID-19 is

$$R_C = \frac{\beta_1(r_1 + \mu)}{(r_1 + \mu + \alpha)(\psi + d_2 + \mu)}.$$

Suppose that  $E_C^* = (S^*, V_C^*, I_C^*)$  endemic equilibrium point of system (2), then by solving system (2) is obtained

$$S^* = \frac{\Lambda}{\beta_C + \alpha + \delta + \mu}, \quad V_C^* = \frac{\alpha \Lambda}{(r_1 + \mu)(\beta_C + \alpha + \delta + \mu)}, \quad I_C^* = \frac{\beta_C \Lambda}{(\psi + d_2 + \mu)(\beta_C + \alpha + \delta + \mu)},$$

with  $\beta_C = \frac{\beta_1}{N_C} I_C^*$ . If  $I_C^*$  substituted to  $\beta_C = \frac{\beta_1}{N} I_C^*$  then obtained

$$\beta_C = \frac{\beta_1(r_1 + \mu) - (\psi + d_2 + \mu)(r_1 + \mu + \alpha)}{(r_1 + \mu)} = \frac{(\psi + d_2 + \mu)(r_1 + \mu + \alpha)}{(r_1 + \mu)} (R_C - 1),$$

this shows that if  $R_C > 1$ , then  $\beta_C$  is positive, so  $I_C^*$  is also positive. In other words, the endemic equilibrium point for the sub-model of the spread of COVID-19 exists and is single if  $R_C > 1$ .

The local stability of the disease-free equilibrium point of System (1) is determined by the

linearization approach. The Jacobian matrix of System (2) at  $E_C^0$  is

$$J(E_C^0) = \begin{pmatrix} -(\alpha + \delta + \mu) & 0 & \frac{\beta_1}{N_C^0} S^0 \\ \alpha & -(\tau_1 + \mu) & 0 \\ 0 & 0 & -(\psi + d_2 + \mu) \end{pmatrix}.$$

It is clear that all the eigenvalues of the matrix  $J(E_C^0)$  are negative. Thus, the disease-free equilibrium point  $E_C^0$  is locally asymptotically stable if  $R_C < 1$ . Next, global stability analysis of the endemic equilibrium point  $E_C^*$  was performed using the Lyapunov method. The Lyapunov function [28] used to determine the global stability of  $E_C^*$  is defined as follows:

$$L(S, V_C, I_C) = \frac{1}{2} \left( (S - S^*) + (V_C - V_C^*) + (I_C - I_C^*) \right)^2.$$

The Lyapunov function  $L$  is a continuously differentiable function and is always positive and zero only at the endemic equilibrium point  $E_C^*$ . If the Lyapunov function  $L$  [28] is derived with respect to  $t$ , then it is obtained

$$\begin{aligned} \frac{dL}{dt} &= \left( (S - S^*) + (V_C - V_C^*) + (I_C - I_C^*) \right) \times \left( \frac{dS}{dt} + \frac{dV_C}{dt} + \frac{dI_C}{dt} \right) \\ &= \left( N_C - \frac{\Lambda - \delta S^* - r_1 V_C^* - (\psi + d_2) I_C^*}{\mu} \right) (\Lambda - \delta S - r_1 V_C - (\psi + d_2) I_C - \mu N_C) \\ &\leq \left( N_C - \frac{\Lambda}{\mu} \right) (\Lambda - \mu N_C) \leq -\frac{(\Lambda - \mu N_C)^2}{\mu} \leq 0. \end{aligned}$$

Since  $R_C > 1$ , there is a unique endemic equilibrium point  $E_C^*$ , and the Lyapunov  $L$  function with  $\frac{dL}{dt} < 0$  is obtained. Thus, it can be concluded that the endemic equilibrium point  $E_C^*$  is globally asymptotically stable.

## 2.2 HIV/AIDS Sub-Model

This case is only concerned with the spread of HIV/AIDS; in this case,  $V_C = I_C = C = R = 0$ . Thus, the sub-model for the case of the spread of COVID-19 is given by the following system of differential equations

$$\left. \begin{aligned} \frac{dS}{dt} &= \Lambda - \left( \alpha + \delta + \frac{\beta_2}{N_H} I_H + \mu \right) S \\ \frac{dP_H}{dt} &= \delta S - (r_2 + \mu) P_H \\ \frac{dI_H}{dt} &= \frac{\beta_2}{N_H} I_H S - (\tau + d_1 + \mu) I_H \\ \frac{dT_H}{dt} &= \tau I_H - (\theta + \mu) T_H \end{aligned} \right\} \quad (3)$$

with  $N_H = S + P_H + I_H + T_H$ . All the equilibrium points of System (3) can be obtained by solving the following system of equations,

$$\frac{dS}{dt} = \frac{dP_H}{dt} = \frac{dI_H}{dt} = \frac{dT_H}{dt} = 0.$$

One of the equilibrium points, which is often referred to as the disease-free equilibrium point ( $E_H^0$ ), is obtained when  $I_H = 0$ . The disease-free equilibrium point for the sub-model of the spread of HIV/AIDS, i.e.,  $E_H^0 = (S^0, P_H^0, I_H^0, T_H^0) = \left( \frac{\Lambda}{\alpha + \delta + \mu}, \frac{\delta \Lambda}{(\alpha + \delta + \mu)(r_2 + \mu)}, 0, 0 \right)$ .

The basic reproduction number of System (3) is determined using the next generation matrix. Based on System (3) the  $F$  and  $V$  matrices are obtained as follows:

$$F = \begin{pmatrix} \frac{\beta_2}{N_H^0} S^0 & 0 \\ N_H^0 & 0 \end{pmatrix}, \quad V = \begin{pmatrix} \tau + d_1 + \mu & 0 \\ 0 & r_2 + \mu \end{pmatrix},$$

with  $N_H^0 = S^0 + P_H^0 + I_H^0 + T_H^0$ .

So that the next-generation matrix is obtained as follows:

$$FV^{-1} = \begin{pmatrix} \frac{\beta_2(r_2 + \mu)}{(r_2 + \mu + \delta)(\tau + d_1 + \mu)} & 0 \\ 0 & 0 \end{pmatrix}.$$

The basic reproduction number of System (3) is the maximum eigenvalue of the  $FV^{-1}$ .

So, the basic reproduction number for the sub-model of the spread of HIV/AIDS is

$$R_H = \frac{\beta_2(r_2 + \mu)}{(r_2 + \mu + \delta)(\tau + d_1 + \mu)}.$$

Suppose that  $E_H^* = (S^*, P_H^*, I_H^*, T_H^*)$  is the endemic equilibrium point of System (3), then solving System (3) is obtained

$$S^* = \frac{\Lambda}{\beta_H + \alpha + \delta + \mu}, \quad P_H^* = \frac{\delta \Lambda}{(r_2 + \mu)(\beta_H + \alpha + \delta + \mu)}, \quad I_H^* = \frac{\beta_H \Lambda}{(\tau + d_1 + \mu)(\beta_H + \alpha + \delta + \mu)}, \quad T_H^* = \frac{\tau}{\theta + \mu} I_H^*,$$

with  $\beta_H = \frac{\beta_2}{N_H} I_H^*$ . If  $I_H^*$  is substituted to  $\beta_H = \frac{\beta_2}{N_H} I_H^*$  we get

$$\beta_H = \frac{\beta_2(r_2 + \mu) - (\tau + d_1 + \mu)(r_2 + \mu + \delta)}{(r_2 + \mu)} = \frac{(\tau + d_1 + \mu)(r_2 + \mu + \delta)}{(r_2 + \mu)} (R_H - 1).$$

This shows that if  $R_H > 1$ , then  $\beta_H$  is positive so that  $I_H^*$  is also positive. In other words, the endemic equilibrium point for the sub-model of the spread of HIV/AIDS exists and is single if  $R_H > 1$ . The local stability of the disease-free equilibrium point of System (3) was determined by

the linearization approach. The Jacobian Matrix of the System (3) at  $E_H^0$  is

$$J(E_H^0) = \begin{pmatrix} -(\alpha + \delta + \mu) & 0 & \frac{\beta_2}{N_H^0} S^0 & 0 \\ \alpha & -(r_2 + \mu) & 0 & 0 \\ 0 & 0 & -(\tau + d_1 + \mu) & 0 \\ 0 & 0 & \tau & -(\theta + \mu) \end{pmatrix}$$

It is clear that all the eigenvalues of the matrix  $J(E_H^0)$  are negative. Thus, the disease-free equilibrium point  $E_H^0$  is locally asymptotically stable if  $R_H < 1$ .

Next, global stability analysis of the endemic equilibrium point  $E_H^*$  was performed using the Lyapunov method. The Lyapunov function used to determine the global stability of  $E_H^*$  is defined as follows [28]:

$$L(S, V_C, I_C) = \frac{1}{2} \left( (S - S^*) + (P_H - P_H^*) + (I_H - I_H^*) + (T_H - T_H^*) \right)^2.$$

The Lyapunov function  $L$  is a continuously differentiable function and is always positive and zero only at the endemic equilibrium point  $E_H^*$ . If the Lyapunov function  $L$  is derived with respect to  $t$ , then it is obtained

$$\begin{aligned} \frac{dL}{dt} &= \left( (S - S^*) + (P_H - P_H^*) + (I_H - I_H^*) + (T_H - T_H^*) \right) \times \left( \frac{dS}{dt} + \frac{dP_H}{dt} + \frac{dI_H}{dt} + \frac{dT_H}{dt} \right) \\ &= \left( N_H - \frac{\Lambda - \alpha S^* - r_2 P_H^* - d_1 I_H^* - \theta T_H^*}{\mu} \right) (\Lambda - \alpha S - r_2 P_H - d_1 I_H - \theta T_H - \mu N_H) \\ &\leq \left( N_H - \frac{\Lambda}{\mu} \right) (\Lambda - \mu N_H) \leq -\frac{(\Lambda - \mu N_H)^2}{\mu} \leq 0 \end{aligned}$$

Since  $R_H > 1$ , there is a unique endemic equilibrium point  $E_H^*$ , and the Lyapunov function  $L$  is obtained with  $\frac{dL}{dt} < 0$ . Thus it can be concluded that the endemic equilibrium point  $E_H^*$  is globally asymptotically stable.

### 2.3 Model of COVID-19 Co-infection with HIV/AIDS

The co-infection model for COVID-19 and HIV/AIDS is as follows:

All equilibrium points of System (1) can be obtained by solving the following system of equations

$$\frac{dS}{dt} = \frac{dV_C}{dt} = \frac{dP_H}{dt} = \frac{dI_C}{dt} = \frac{dI_H}{dt} = \frac{dC}{dt} = \frac{dT_H}{dt} = \frac{dR}{dt} = 0.$$

The disease-free equilibrium point of System (4) is  $E_{CH}^0 = (S^0, V_C^0, P_H^0, 0, 0, 0, 0, R^0)$  with,

$$S^0 = \frac{\Lambda}{\alpha + \delta + \mu}, V_C^0 = \frac{\alpha \Lambda}{(\alpha + \delta + \mu)(r_1 + \mu)}, P_H^0 = \frac{\delta \Lambda}{(\alpha + \delta + \mu)(r_2 + \mu)}, R^0 = \frac{r_1 V_C^0 + r_2 P_H^0}{\mu}.$$

The basic reproduction number of System (1) is determined using the next-generation matrix.

Based on System (1), the  $F$  and  $V$  matrices are obtained as follows:

$$F = \begin{pmatrix} \frac{\beta_1 S^0}{N^0} & 0 & 0 \\ 0 & \frac{\beta_2 S^0}{N^0} & 0 \\ 0 & 0 & 0 \end{pmatrix}, \quad V = \begin{pmatrix} \psi + d_2 + \mu & 0 & 0 \\ 0 & \tau + d_1 + \mu & 0 \\ 0 & 0 & \sigma + d_3 + \mu \end{pmatrix}$$

with  $N^0 = S^0 + V_C^0 + P_H^0 + I_C^0 + I_H^0 + T_H^0 + R^0$ . So that the next-generation matrix is obtained as follows:

$$FV^{-1} = \begin{pmatrix} \frac{\beta_1 S^0}{(\psi + d_2 + \mu)N^0} & 0 & 0 \\ 0 & \frac{\beta_2 S^0}{(\tau + d_1 + \mu)N^0} & 0 \\ 0 & 0 & 0 \end{pmatrix}$$

The basic reproduction number of System (1) is the maximum eigenvalue of the  $FV^{-1}$ . So, the basic reproduction number for the co-infection model of COVID-19 and HIV/AIDS is

$$\mathfrak{R}_{CH} = \max \left\{ \frac{\beta_1 S^0}{(\psi + d_2 + \mu)N^0}, \frac{\beta_2 S^0}{(\tau + d_1 + \mu)N^0} \right\}.$$

The local stability of the disease-free equilibrium point of System (1) is determined using the Jacobian matrix at  $E_{CH}^0$  as follows

$$J(E_{CH}^0) = \begin{pmatrix} -(\alpha + \delta + \mu) & 0 & 0 & J_{14} & J_{15} & J_{16} & 0 & 0 \\ \alpha & -(\tau_1 + \mu) & 0 & 0 & J_{25} & J_{26} & 0 & 0 \\ \delta & 0 & -(\tau_2 + \mu) & J_{34} & 0 & J_{36} & 0 & 0 \\ 0 & 0 & 0 & J_{44} & 0 & J_{46} & 0 & 0 \\ 0 & 0 & 0 & 0 & J_{55} & J_{56} & 0 & 0 \\ 0 & 0 & 0 & 0 & 0 & J_{66} & \theta & 0 \\ 0 & 0 & 0 & 0 & \tau & \sigma & -(\theta + \mu) & 0 \\ 0 & r_1 & r_2 & \psi & 0 & 0 & 0 & -\mu \end{pmatrix}$$

So that the characteristic equation is obtained as follows

$$(\lambda + \mu)(\lambda + r_1 + \mu)(\lambda + r_2 + \mu)(\lambda + \alpha + \delta + \mu)(\lambda - J_{44})(\lambda^3 + a_2\lambda^2 + a_1\lambda + a_0) = 0,$$

with

$$J_{14} = \frac{\beta_1 S^0}{N^0}, J_{15} = \frac{\beta_2 S^0}{N^0}, J_{16} = \frac{(\beta_1 \gamma_1 + \beta_2 \gamma_2) S^0}{N^0}, J_{25} = \frac{\varphi \beta_2 V^0}{N^0}, J_{26} = \frac{\gamma_2 \beta_2 V^0}{N^0}, J_{34} = \frac{\omega \beta_1 P^0}{N^0},$$

$$J_{36} = \frac{\omega \beta_1 \gamma_1 P^0}{N^0}, J_{44} = (R_{CH} - 1) - \frac{\omega \beta_1 P^0}{N^0}, J_{46} = \frac{\beta_1 \gamma_1 S^0}{N^0} + \frac{\omega \beta_1 \gamma_1 P^0}{N^0}, J_{55} = \frac{\beta_2 S^0}{N^0} - (\tau + d_1 + \mu),$$

$$J_{56} = \frac{\beta_1 \gamma_1 S^0}{N^0} + \frac{\varphi \beta_1 \gamma_1 V^0}{N^0}, J_{66} = -(\tau + d_3 + \mu).$$

Clearly that all eigenvalues of  $J(E_{CH}^0)$  are negative if  $J_{44} < 0$ . It means that if  $R_{CH} < 1$ , then the endemic equilibrium point  $E_{CH}^0$  is locally asymptotically stable.

### 3. AN OPTIMAL CONTROL OF MODEL OF THE SPREAD OF COVID-19 CO-INFECTION WITH HIV/AIDS AND NUMERICAL SIMULATION

In the dynamic model of co-infection spread involving both COVID-19 and HIV/AIDS, various controls are implemented. By utilizing the system of equations (1) and applying controls  $u_1, u_2, u_3$ , and  $u_4$ , we arrive at the following set of equations.

$$\left. \begin{aligned} \frac{dS}{dt} &= \Lambda - (\alpha + \delta + (1 - u_1)\beta_C + (1 - u_2)\beta_H + \mu)S \\ \frac{dV_C}{dt} &= \alpha S - (r_1 + \varphi(1 - u_2)\beta_H + \mu)V_C \\ \frac{dP_H}{dt} &= \delta S - (r_2 + \omega(1 - u_1)\beta_C + \mu)P_H \\ \frac{dI_C}{dt} &= (1 - u_1)\beta_C S + \omega(1 - u_1)\beta_C P_H - ((1 + u_3)\psi + \xi(1 - u_2)\beta_H + d_2 + \mu)I_C \\ \frac{dI_H}{dt} &= (1 - u_2)\beta_H S + \varphi(1 - u_2)\beta_H V_C - (\tau + \rho(1 - u_1)\beta_C + d_1 + \mu)I_H \\ \frac{dC}{dt} &= \xi(1 - u_2)\beta_H I_C + \rho(1 - u_1)\beta_C I_H + \theta T_H - ((1 + u_4)\sigma + d_3 + \mu)C \\ \frac{dT_H}{dt} &= \tau I_H + (1 + u_4)\sigma C - (\theta + \mu)T_H \\ \frac{dR}{dt} &= r_1 V_C + r_2 P_H + (1 + u_3)\psi I_C - \mu R \end{aligned} \right\} \quad (4)$$

One of these controls is the preventive measure with counseling, denoted as  $u_1$ , aimed at averting COVID-19 infection in susceptible individuals. Another preventive measure with counseling, denoted as  $u_2$ , targets individuals from vulnerable subpopulations to prevent HIV/AIDS infection. Furthermore, control  $u_3$  focuses on treating individuals infected with COVID-19, with efforts directed towards expediting their recovery. Additionally, control  $u_4$  is implemented to address the treatment of individuals who are co-infected with both COVID-19 and HIV/AIDS, aiming to accelerate their recovery from COVID-19.

The goal of optimal control and prevention is to minimize the cost of handling and reduce the spread of COVID-19, HIV/AIDS and COVID-19 and HIV/AIDS co-infection. The functional objective of the control review of prevention and treatment of the system is

$$J = \min_u \int_{t_0}^{t_f} (A_1 I_C(t) + A_2 I_H(t) + A_3 C(t) + A_4 u_1^2(t) + A_5 u_2^2(t) + A_6 u_3^2(t) + A_7 u_4^2(t)) dt. \quad (5)$$

Based on equations (4) and (5) the Hamiltonian equation [29] is formed:

$$\begin{aligned}
H = & A_1 I_C(t) + A_2 I_H(t) + A_3 C(t) + A_4 u_1^2(t) + A_5 u_2^2(t) + A_6 u_3^2(t) + A_7 u_4^2(t) \\
& + \lambda_1 (\Lambda - (\alpha + \delta + (1 - u_1)\beta_C + (1 - u_2)\beta_H + \mu)S) \\
& + \lambda_2 (\alpha S - (r_1 + \varphi(1 - u_2)\beta_H + \mu)V_C) \\
& + \lambda_3 (\delta S - (r_2 + \omega(1 - u_1)\beta_C + \mu)P_H) \\
& + \lambda_4 ((1 - u_1)\beta_C S + \omega(1 - u_1)\beta_C P_H - ((1 + u_3)\psi + \xi(1 - u_2)\beta_H + d_2 + \mu)I_C) \\
& + \lambda_5 ((1 - u_2)\beta_H S + \varphi(1 - u_2)\beta_H V_C - (\tau + \rho(1 - u_1)\beta_C + d_1 + \mu)I_H) \\
& + \lambda_6 (\xi(1 - u_2)\beta_H I_C + \rho(1 - u_1)\beta_C I_H + \theta T_H - ((1 + u_4)\sigma + d_3 + \mu)C) \\
& + \lambda_7 (\tau I_H + (1 + u_4)\sigma C - (\theta + \mu)T_H) \\
& + \lambda_8 (r_1 V_C + r_2 P_H + (1 + u_3)\psi I_C - \mu R)
\end{aligned} \tag{6}$$

### Teorema

Based on the system of state equations (4), objective functional equations (5), and the Hamiltonian function (6), the co-state function system and optimal control are obtained as follows.

$$\begin{aligned}
\lambda'_1 &= (\lambda_1 - \lambda_2)\alpha + (\lambda_1 - \lambda_3)\delta + (\lambda_1 - \lambda_4)(1 - u_1)\beta_C + (\lambda_1 - \lambda_5)(1 - u_2)\beta_H + \lambda_1\mu \\
\lambda'_2 &= (\lambda_2 - \lambda_5)\varphi(1 - u_2)\beta_H + (\lambda_2 - \lambda_8)r_1 + \lambda_2\mu \\
\lambda'_3 &= (\lambda_3 - \lambda_4)\omega(1 - u_1)\beta_C + (\lambda_3 - \lambda_8)r_2 + \lambda_3\mu \\
\lambda'_4 &= -A_1 + (\lambda_1 - \lambda_4)(1 - u_1)\frac{\beta_C S}{N} + (\lambda_3 - \lambda_4)\omega(1 - u_1)\frac{\beta_C P_H}{N} + (\lambda_4 - \lambda_8)(1 + u_3)\psi \\
& + (\lambda_4 - \lambda_6)\xi(1 - u_2)\beta_H + (\lambda_5 - \lambda_6)\rho(1 - u_1)\frac{\beta_1 I_H}{N} + \lambda_4(d_2 + \mu) \\
\lambda'_5 &= -A_2 + (\lambda_1 - \lambda_5(1 - u_2))\frac{\beta_H S}{N} + (\lambda_2 - \lambda_5)\omega(1 - u_2)\frac{\beta_H V_C}{N} + (\lambda_4 - \lambda_6)(1 + u_3)\frac{\beta_2 I_C}{N} \\
& + (\lambda_5 - \lambda_7)\tau + (\lambda_5 - \lambda_6)\rho(1 - u_1)\beta_C + \lambda_5(d_1 + \mu) \\
\lambda'_6 &= -A_3 + (\lambda_6 - \lambda_7)(1 + u_4)\sigma + \lambda_6(d_3 + \mu) \\
\lambda'_7 &= (\lambda_7 - \lambda_6)\theta + \lambda_7\mu \\
\lambda'_8 &= \lambda_8\mu,
\end{aligned}$$

with the condition of transversality  $\lambda_i(t_f) = 0$ ,  $i = 1, 2, 3, 4, 5, 6, 7, 8$ , and optimal control

$$\begin{aligned}
u_1^* &= \frac{(\lambda_4 - \lambda_1)\beta_C S + (\lambda_4 - \lambda_3)\omega\beta_C P_H + (\lambda_6 - \lambda_5)\rho\beta_C I_H}{2A_4} \\
u_2^* &= \frac{(\lambda_5 - \lambda_1)\beta_H S + (\lambda_5 - \lambda_2)\varphi\beta_H V_C + (\lambda_6 - \lambda_4)\xi\beta_H I_C}{2A_5}
\end{aligned}$$

$$u_3^* = \frac{(\lambda_4 - \lambda_8)\psi I_C}{2A_6}$$

$$u_4^* = \frac{(\lambda_6 - \lambda_7)\sigma C}{2A_7} .$$

Proof

By using the Pontryagin's Maximum Principle [29], the partial time derivative of each co-state is the negative of the partial time derivative of the corresponding state Hamiltonian. It is obtained as follows:

$$\lambda_1' = -\frac{\partial H}{\partial S}$$

$$= (\lambda_1 - \lambda_2)\alpha + (\lambda_1 - \lambda_3)\delta + (\lambda_1 - \lambda_4)(1 - u_1)\beta_C + (\lambda_1 - \lambda_5)(1 - u_2)\beta_H + \lambda_1\mu$$

$$\lambda_2' = -\frac{\partial H}{\partial V_C} = (\lambda_2 - \lambda_5)\varphi(1 - u_2)\beta_H + (\lambda_2 - \lambda_8)r_1 + \lambda_2\mu$$

$$\lambda_3' = -\frac{\partial H}{\partial P_H} = (\lambda_3 - \lambda_4)\omega(1 - u_1)\beta_C + (\lambda_3 - \lambda_8)r_2 + \lambda_3\mu$$

$$\lambda_4' = -\frac{\partial H}{\partial I_C} = -A_1 + (\lambda_1 - \lambda_4)(1 - u_1)\frac{\beta_C S}{N} + (\lambda_3 - \lambda_4)\omega(1 - u_1)\frac{\beta_C P_H}{N} + (\lambda_4 - \lambda_8)(1 + u_3)\psi$$

$$+ (\lambda_4 - \lambda_6)\xi(1 - u_2)\beta_H + (\lambda_5 - \lambda_6)\rho(1 - u_1)\frac{\beta_C I_H}{N} + \lambda_4(d_2 + \mu)$$

$$\lambda_5' = -\frac{\partial H}{\partial I_H} = -A_2 + (\lambda_1 - \lambda_5)(1 - u_2)\frac{\beta_H S}{N} + (\lambda_2 - \lambda_5)\omega(1 - u_2)\frac{\beta_H V_C}{N}$$

$$+ (\lambda_5 - \lambda_7)\tau + (\lambda_5 - \lambda_6)\rho(1 - u_1)\beta_C + \lambda_5(d_1 + \mu)$$

$$\lambda_6' = -\frac{\partial H}{\partial C} = -A_3 + (\lambda_6 - \lambda_7)(1 + u_4)\sigma + \lambda_6(d_3 + \mu)$$

$$\lambda_7' = -\frac{\partial H}{\partial T_H} = (\lambda_7 - \lambda_6)\theta + \lambda_7\mu$$

$$\lambda_8' = -\frac{\partial H}{\partial R} = \lambda_8\mu,$$

with transversality condition,  $\lambda_i(t_f) = 0$ ,  $i = 1, 2, 3, 4, 5, 6, 7, 8$ .

While the optimal control conditions,  $\frac{\partial H}{\partial u_1} = \frac{\partial H}{\partial u_2} = \frac{\partial H}{\partial u_3} = \frac{\partial H}{\partial u_4} = 0$ , obtained

$$u_1^* = \frac{(\lambda_4^* - \lambda_1^*)\beta_C S + (\lambda_4^* - \lambda_3^*)\omega\beta_C P_H + (\lambda_6^* - \lambda_5^*)\rho\beta_C I_H}{2A_4}$$

$$u_2^* = \frac{(\lambda_5^* - \lambda_1^*)\beta_H S + (\lambda_5^* - \lambda_2^*)\varphi\beta_H V_C + (\lambda_6^* - \lambda_4^*)\xi\beta_H I_C}{2A_5}$$

$$u_3^* = \frac{(\lambda_4^* - \lambda_8^*)\psi I_C}{2A_6}$$

$$u_4^* = \frac{(\lambda_6^* - \lambda_7^*)\sigma C}{2A_7}.$$

Each optimal control can be stated according to its limitations as follows:

$$u_1^* = \max \left\{ 0, \min \left\{ \frac{(\lambda_4^* - \lambda_1^*)\beta_C S + (\lambda_4^* - \lambda_3^*)\omega\beta_C P_H + (\lambda_6^* - \lambda_5^*)\rho\beta_C I_H}{2A_4}, 1 \right\} \right\}$$

$$u_2^* = \max \left\{ 0, \min \left\{ \frac{(\lambda_5^* - \lambda_1^*)\beta_H S + (\lambda_5^* - \lambda_2^*)\varphi\beta_H V_C + (\lambda_6^* - \lambda_4^*)\xi\beta_H I_C}{2A_5}, 1 \right\} \right\}$$

$$u_3^* = \max \left\{ 0, \min \left\{ \frac{(\lambda_4^* - \lambda_8^*)\psi I_C}{2A_6}, 1 \right\} \right\}$$

$$u_4^* = \max \left\{ 0, \min \left\{ \frac{(\lambda_6^* - \lambda_7^*)\sigma C}{2A_7}, 1 \right\} \right\}. \quad \square$$

### 3.1 The Model's Solution with and Without Control

Several simulations are performed using parameters' value in Table 1 and initial conditions of each subpopulation based on Indonesian data on March 14, 2022:  $S(0) = 208,265,720$ ,  $V_C(0) = 151,693,762$ ,  $P_H(0) = 254,300$ ,  $I_C(0) = 312,958$ ,  $I_H(0) = 328,581$ ,  $C(0) = 67$ ,  $T_H(0) = 60$ ,  $R(0) = 5,434,729$ . First, we present the time series of the model's solution in Figure 2. The susceptible and vaccinated subpopulations are declining, meanwhile the recovered subpopulation grows until reaching the steady state. On the other hand, the infected subpopulations of COVID-19, HIV/AIDS, and co-infection grows at first until reaching their peak and then declines resulting zero infection cases.

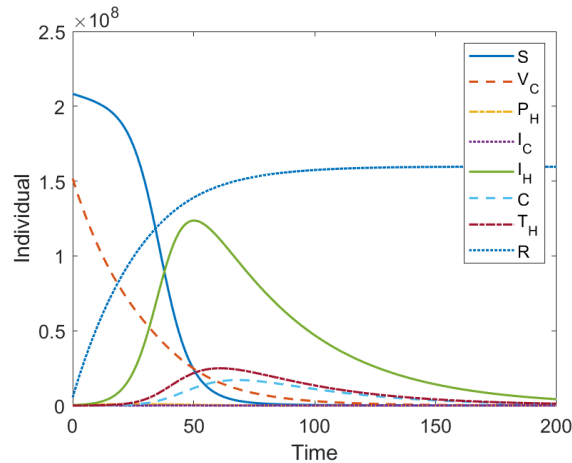
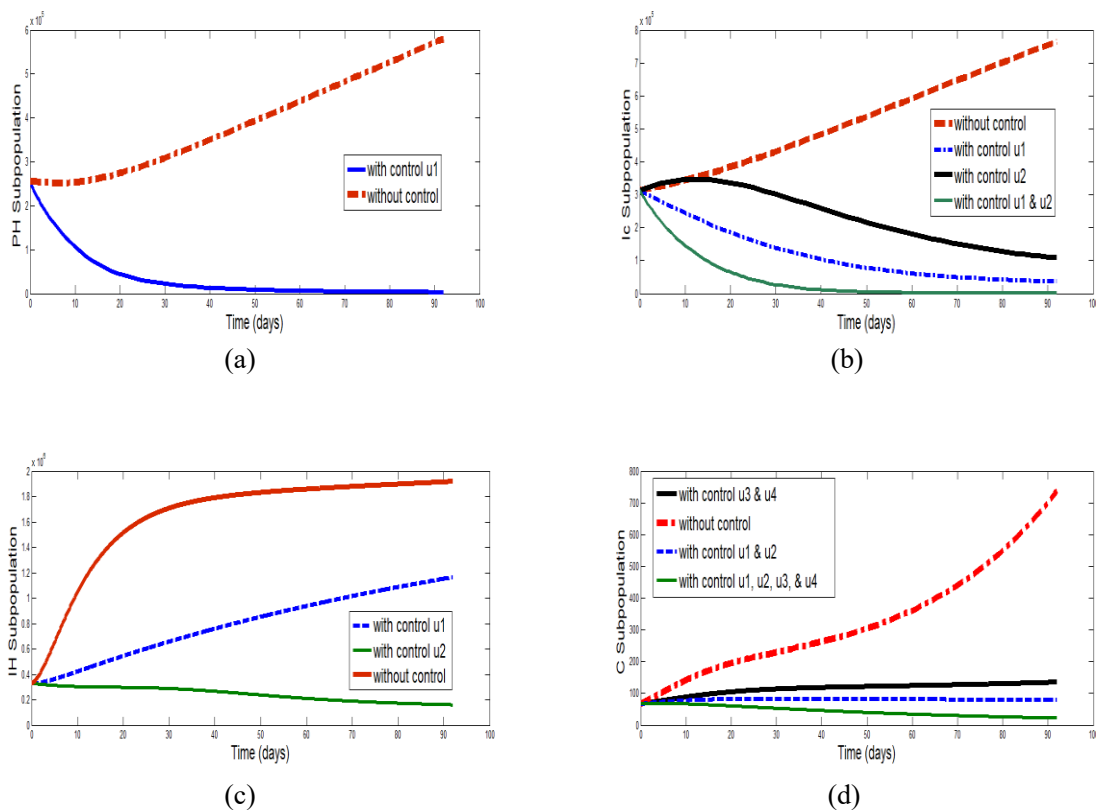


Figure 2. Plot of each subpopulation over time.

To determine the influence of optimal prevention and treatment intervention controls on the dynamics of COVID-19 co-infection with HIV/AIDS, the following controls are considered: Prevention control with counseling to prevent COVID-19 infection ( $u_1$ ). Prevention control with counseling to prevent HIV/AIDS infection ( $u_2$ ). Treatment control for individuals infected with COVID-19 ( $u_3$ ). Treatment control for individuals co-infected with both COVID-19 and HIV/AIDS ( $u_4$ ). Control  $u_1$  prevents subpopulation  $S$  from entering  $I_C$ , prevents subpopulation  $P_H$  from entering  $I_C$ , and prevents subpopulation  $I_H$  from entering  $C$ . Control  $u_2$  prevents subpopulation  $S$  from entering  $I_H$ , prevents subpopulation  $V_C$  from entering  $I_H$ , and prevents subpopulation  $I_C$  from entering  $C$ . Control  $u_3$  increases the transition of subpopulation  $I_C$  to  $R$ , and control  $u_4$  increases the transition of subpopulation  $C$  to  $T_H$ .

The solutions for state, co-state, and the optimal prevention and treatment controls were obtained using the Pontryagin's Maximum Principle [29]. The spread of subpopulations with intervention controls and without controls can be seen in Figure 3.



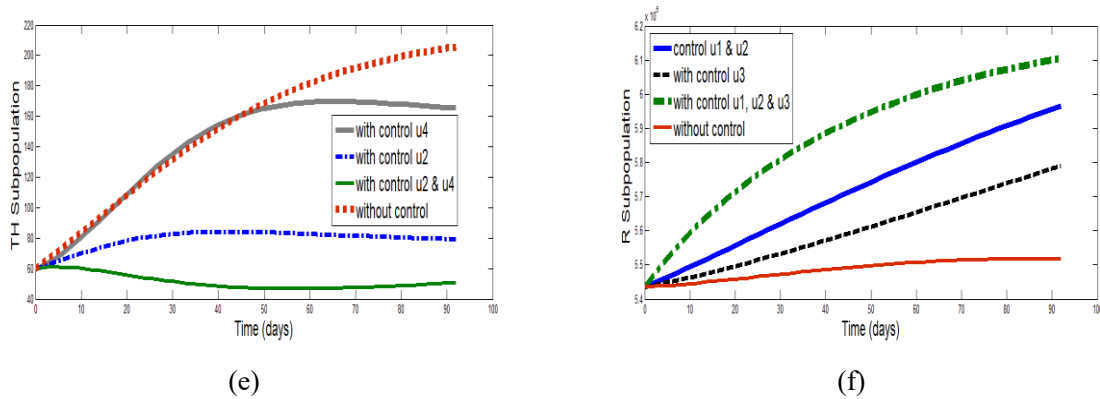


Figure 3. Dynamics of  $P_H$ ,  $I_C$ ,  $I_H$ ,  $C$ ,  $T_H$ , and  $R$  subpopulations with and without control.

Based on Figure 3(a), with control  $u_1$ , the number of individuals in the  $P_H$  subpopulation decreases, while without control, the number of individuals in the  $P_H$  subpopulation increases from the initial time until  $t = 92$  days. In Figure 3(b), it is evident that without control, the number of individuals in the  $I_C$  subpopulation increases, whereas with control  $u_1$  and/or  $u_2$ , the number of individuals in the  $I_C$  subpopulation decreases from the initial time until  $t = 92$  days. Action with control  $u_1$  is more effective in reducing the number of individuals in the  $I_C$  subpopulation compared to control  $u_2$ . In Figure 3(c), the number of individuals in the  $I_H$  subpopulation increases continuously without control from the initial time until  $t = 92$  days, while with control  $u_1$ , the increase is gradual, but with control  $u_2$ , it already decreases. In Figure 3(d), the number of individuals in the  $C$  subpopulation increases without control; with treatment controls  $u_3$  and  $u_4$ , the increase is still gradual, while with prevention controls  $u_1$  and  $u_2$ , it follows a monotonic trend, and with combined prevention and treatment controls, it decreases from the initial time until  $t = 92$  days.

In Figure 3(e), it can be observed that the number of individuals in the  $T_H$  subpopulation increases without control and with control  $u_4$ . In actions with  $u_2$  control, the increase is gradual from the initial time until  $t = 30$  days and from  $t = 30$  days until  $t = 92$  days; it follows a monotonic trend. However, with combined controls  $u_2$  and  $u_4$ , it decreases slowly from the initial time until  $t = 92$  days. In Figure 3(f), the number of individuals in the  $R$  subpopulation increases from the

initial time until  $t = 92$  days. The combined use of controls  $u_1$ ,  $u_2$ , and  $u_3$  is more effective than using them individually. Additionally, prevention controls  $u_1$  and  $u_2$  are more effective in increasing the number of individuals in the R subpopulation from the initial time until  $t = 92$  days compared to treatment control  $u_3$ .

### 3.2 Sensitivity Analysis

To evaluate which parameter of the model has the most proportional impact on the disease spread, it is important to calculate the elasticity index of the basic reproduction number which is defined as follows

$$\Upsilon_q = \frac{\partial R_0}{\partial q} \times \frac{q}{R_0}$$

where  $q$  is the parameter and  $R_0$  is the basic reproduction number. The advantage of the elasticity index calculation is that we can find another way to control the disease spread by paying attention to the most sensitive parameter.

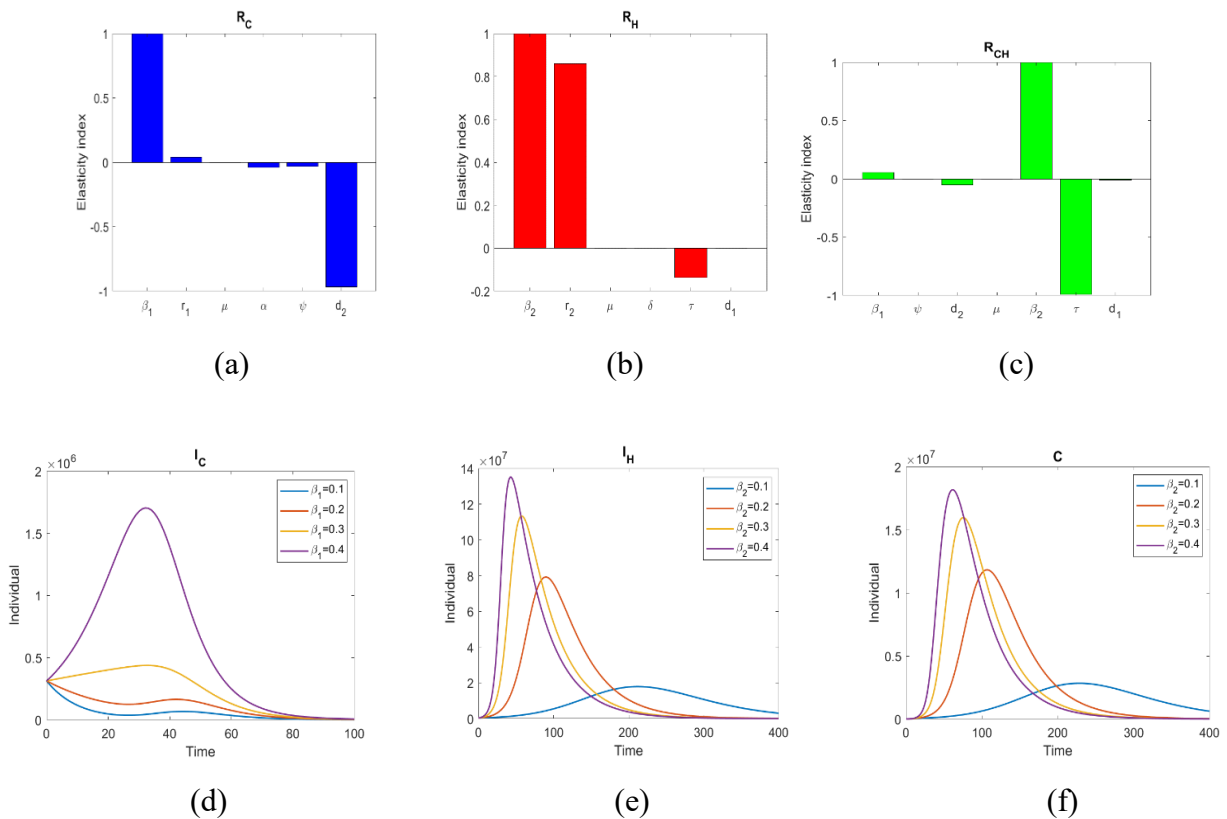


Figure 4. (a-c) Elasticity index of  $R_C$ ,  $R_H$ , and  $R_{CH}$ . (d-f) The sensitivity of parameters  $\beta_1$  and  $\beta_2$  on the dynamics of the infected subpopulations  $I_C$ ,  $I_H$ , and  $C$ .

## SPREAD OF COVID-19 CO-INFECTION WITH HIV/AIDS

The elasticity index of the COVID-19 basic reproduction number  $R_C$ , the HIV/AIDS reproduction number  $R_H$ , and the co-infection  $\mathfrak{R}_{CH}$  is given in Figure 4a-c. In the case of  $R_C$ , it is found that parameter  $\beta_1$  and followed by  $d_2$  are the most sensitive. In the case of  $R_H$ , the parameter  $\beta_2$  is the most sensitive and it is followed by  $r_2$ . Thus, to gain maximal result in controlling the COVID-19 spread, we should reduce the contact rate  $\beta_1$ , for example by social distancing; while to gain maximal result in reducing the HIV/AIDS spread, we should reduce the contact rate  $\beta_2$ , for example by using condoms when doing sex. In the co-infection case, the simulation shows that the parameters  $\beta_2$  and  $\tau$  are the most sensitive. Thus, in order to reduce the co-infection spread, we should pay attention to the reducing the contact rate of HIV/AIDS patients or increasing the their treatment rate. In Figure 4d-f, we have the sensitivity of parameter  $\beta_1$  on the dynamics of the infected COVID-19  $I_C$ , and the sensitivity of parameter  $\beta_2$  on the dynamics of the infected HIV/AIDS  $I_H$  and co-infected  $C$ . The result is similar to the elasticity index analysis, that higher contact rate will produce higher numbers of the infected subpopulations.

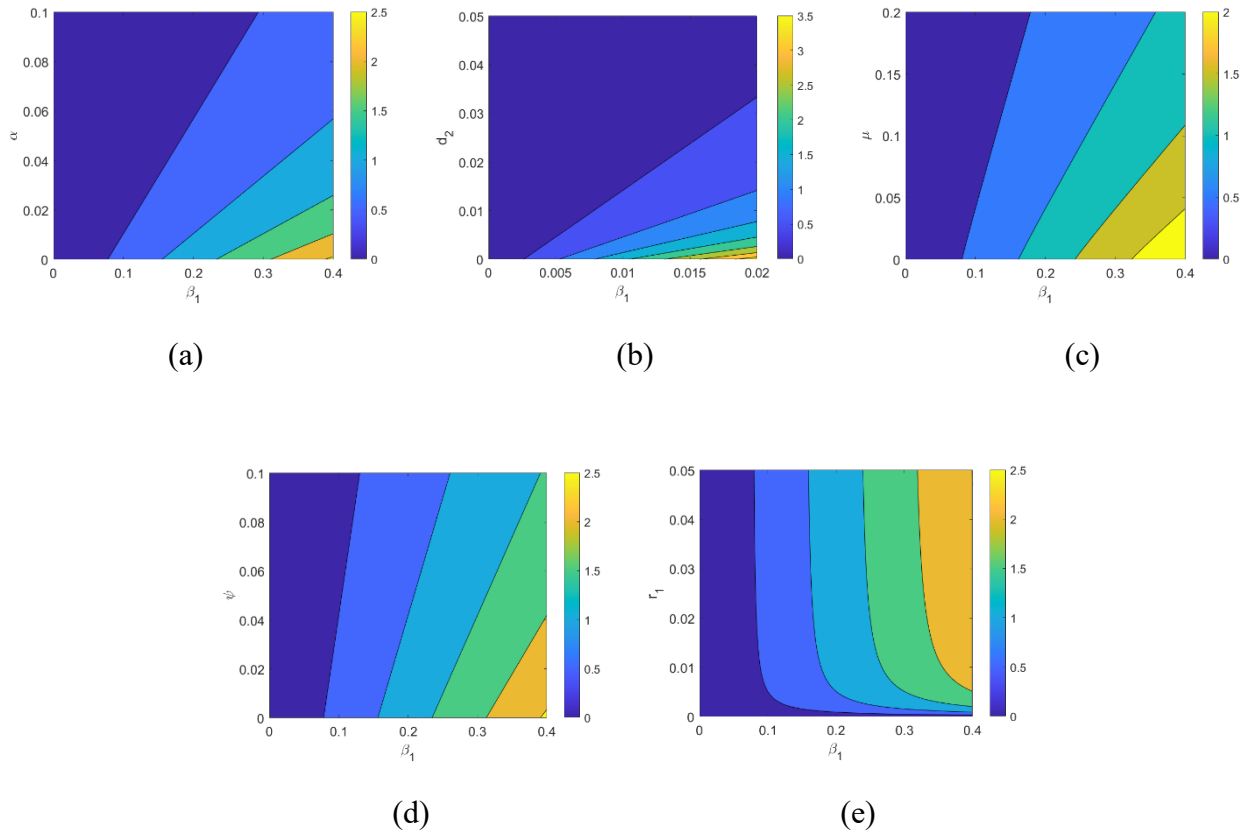


Figure 5. Contour plots of  $R_C$  as a function of the contact rate  $\beta_1$  and other parameters.

Consider the basic reproduction numbers as a function of the model's parameters. First, we view  $R_C = \frac{\beta_1(r_1+\mu)}{(r_1+\mu+\alpha)(\psi+d_2+\mu)}$  as a function of  $\beta_1$  and other parameters. We want to know the simultaneous influence of contact rate  $\beta_1$  with other parameters on the COVID-19 spread. To do this, we plot the contour of  $R_C$ , and the result is given in Figure 5. All the figures conclude that higher contact rate influences the disease to spread. To control the spread, the parameters  $\alpha$ ,  $d_2$ ,  $\mu$ , and  $\psi$  should have higher value, or  $r_1$  should have very small value.

Second, consider  $R_H = \frac{\beta_2(r_2+\mu)}{(r_2+\mu+\delta)(\tau+d_1+\mu)}$  as a function of contact rate  $\beta_2$  and other parameters. Similar as before, the contour plot of  $R_H$  is plotted, and we present it in Figure 6. The result is similar to the case of COVID-19 spread, that higher value of contact rate will make HIV/AIDS to spread. In order to control the disease's spread, we should have higher value of parameters  $d_1$ ,  $\delta$ ,  $\mu$ , and  $\tau$ , or very small value of  $r_2$ .

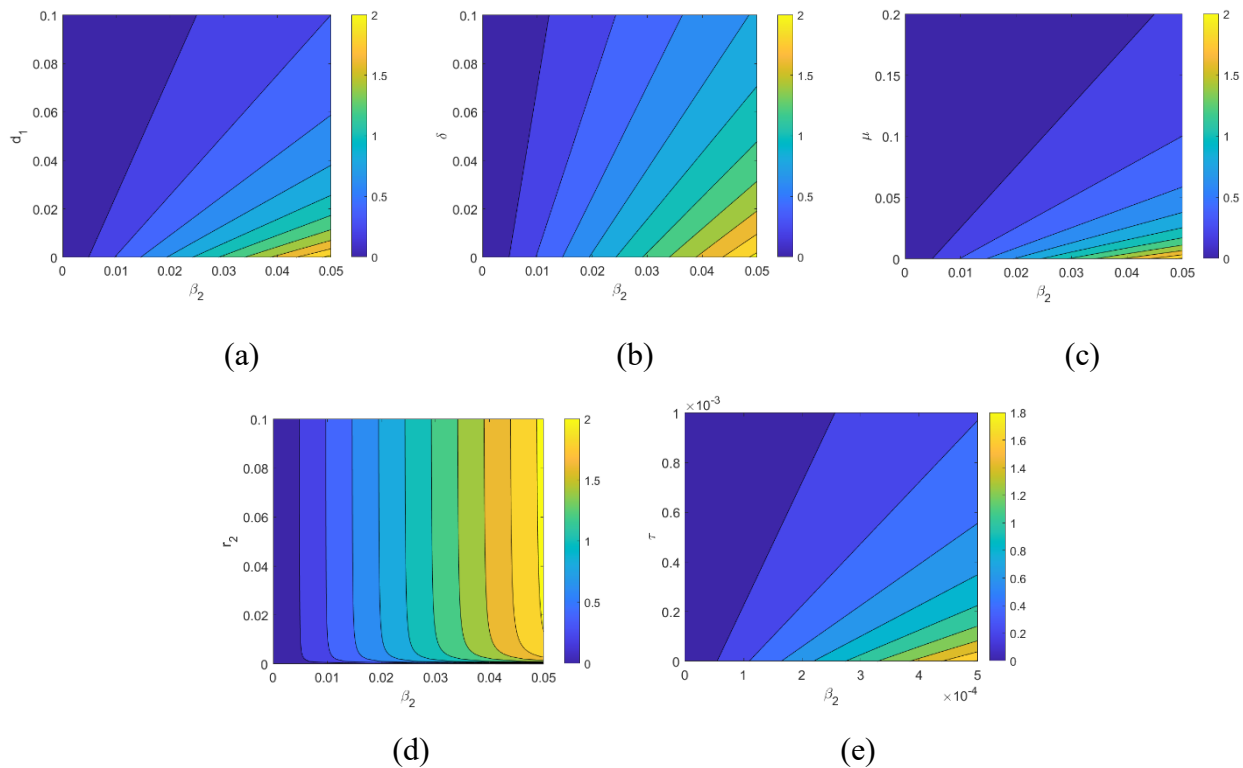


Figure 6. Contour plots of  $R_H$  as a function of the contact rate  $\beta_2$  and other parameters.

The last, suppose  $\mathfrak{R}_{CH} = \max\left\{\frac{\beta_1 S^0}{(\psi+d_2+\mu)N^0}, \frac{\beta_2 S^0}{(\tau+d_1+\mu)N^0}\right\}$  as a function of two parameters. Its contour plot is given in Figure 7. We have an interesting result that at some parameter-space the contour plot produces a discontinuous display. It is resulted from the maximum operator. By Figure 6a, it is obtained that the influence of HIV/AIDS contact rate ( $\beta_2$ ) is larger than COVID-19 contact rate ( $\beta_1$ ). In Figure 7b, the smaller value of  $\beta_2$  and the higher value of  $d_2$  will decrease simultaneously the coinfection disease.

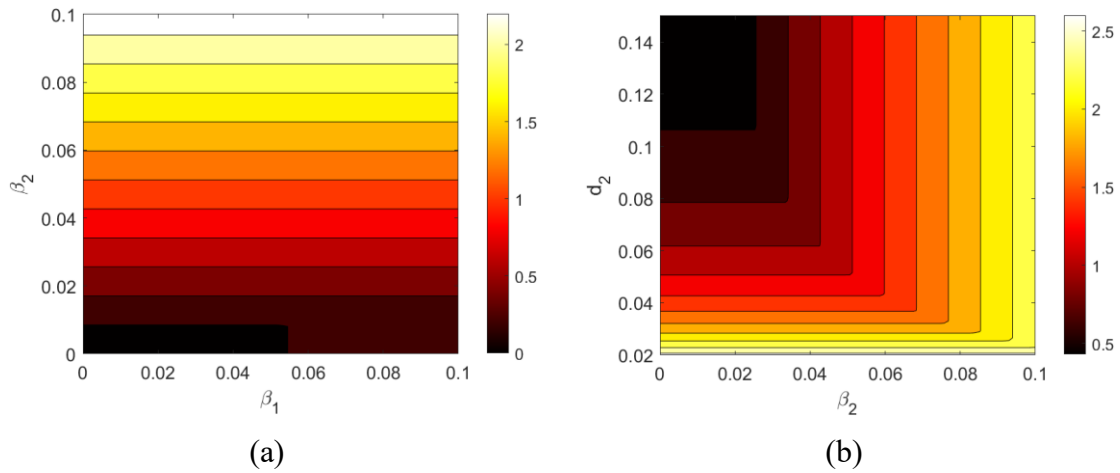


Figure 7. Contour plot of  $\mathfrak{R}_{CH}$  as a function of  $\beta_2$  with  $\beta_1$  and  $d_2$ .

#### 4. CONCLUSION

The model studied in this research is an extension of Teklu's study (2023) [24], incorporating vaccination parameters and investigating prevention controls  $u_1$ ,  $u_2$ , and treatment controls  $u_3$  and  $u_4$ . Based on the model analysis, non-endemic equilibrium points and endemic equilibrium points are obtained for each sub-model: COVID-19, HIV/AIDS, and COVID-19 co-infection with HIV/AIDS. To assess whether the number of infected individuals is increasing or decreasing in the COVID-19, HIV/AIDS, and co-infection sub-models, the basic reproduction number for each sub-model is determined. The local stability of the non-endemic equilibrium points in each sub-model, i.e., COVID-19 sub-model ( $E_C^0$ ), HIV/AIDS submodel ( $E_H^0$ ), and COVID-19 co-infection with HIV/AIDS sub-model ( $E_{CH}^0$ ), is analyzed based on the eigenvalues of the Jacobian matrix. The global stability of the endemic equilibrium points in each submodel, i.e., COVID-19 submodel ( $E_C^*$ ), HIV/AIDS sub-model ( $E_H^*$ ), and COVID-19 co-infection with HIV/AIDS sub-model ( $E_{CH}^*$ )

is assessed using the Lyapunov method. Sensitivity analysis reveals critical parameters strongly influencing the reduction or increase in the spread of COVID-19-HIV/AIDS co-infection.

Based on the study of optimal controls in the model of COVID-19 co-infection with HIV/AIDS, the system of differential equations for the co-state of the disease co-infection model is obtained. The optimal prevention control  $u_1$  is more efficient in reducing the number of individuals infected with COVID-19 compared to treatment controls  $u_3$  and  $u_4$ . Moreover, the optimal prevention control  $u_2$  is more efficient in controlling the spread of HIV/AIDS compared to without control.

Another way to control the spread of COVID-19 and HIV/AIDS co-infection is by analyzing the sensitivity of the basic reproduction number. Following the elasticity index analysis, it is found that parameter  $\beta_1$  is the most sensitive to be controlled in the case of COVID-19 infection only. Thus, to gain maximal result in controlling the COVID-19 spread, we should reduce the contact rate  $\beta_1$ , for example by social distancing. In the case of HIV/AIDS infection only, the parameter  $\beta_2$  is the most sensitive. And to gain maximal result in reducing the HIV/AIDS spread, we should reduce the contact rate  $\beta_2$ , for example by using condoms when doing sex. In the co-infection case, the simulation shows that the parameters  $\beta_2$  and  $\tau$  are the most sensitive. Thus, in order to reduce the co-infection's spread, we should pay attention to the reducing the contact rate of HIV/AIDS patients or increasing their treatment rate. Based on the study model in this study, it can be developed on the spread of HIV/AIDS co-infection with tuberculosis, malaria, influenza and other infectious diseases. Analysis models can be used with other methods, namely: fractional or stochastic.

#### **ACKNOWLEDGMENT**

The authors would like to thank Kemenristek Dikti for giving Higher Education Grants of College Leading Basic Research for Fiscal Year 2023, which were funded by LPPM Universitas Cenderawasih.

#### **CONFLICT OF INTERESTS**

The authors declare that there is no conflict of interests.

**REFERENCES**

- [1] WHO, Clinical management of COVID-19 patients: living guideline, (2022).  
<https://app.magicapp.org/#/guideline/6470>.
- [2] UNAIDS, The path that ends AIDS: UNAIDS Global AIDS Update 2023, (2023).  
<https://www.unaids.org/en/resources/documents/2023/global-aids-update-2023>.
- [3] F. Ndaïrou, I. Area, J.J. Nieto, et al. Mathematical modeling of COVID-19 transmission dynamics with a case study of Wuhan, *Chaos Solitons Fractals*. 135 (2020), 109846. <https://doi.org/10.1016/j.chaos.2020.109846>.
- [4] I. Ahmed, G.U. Modu, A. Yusuf, et al. A mathematical model of Coronavirus Disease (COVID-19) containing asymptomatic and symptomatic classes, *Results Phys*. 21 (2021), 103776.  
<https://doi.org/10.1016/j.rinp.2020.103776>.
- [5] J. Nainggolan, M.F. Ansori, Stability and sensitivity analysis of the COVID-19 spread with comorbid diseases, *Symmetry*. 14 (2022), 2269. <https://doi.org/10.3390/sym14112269>.
- [6] J. Nainggolan, J. Harianto, H. Tasman, An optimal control of prevention and treatment of COVID-19 spread in Indonesia, *Commun. Math. Biol. Neurosci*. 2023 (2023), 3. <https://doi.org/10.28919/cmbn/7820>.
- [7] E.O. Omondi, R.W. Mbogo, L.S. Luboobi, A mathematical model of HIV transmission between commercial sex workers and injection drug users, *Res. Math*. 9 (2022), 2082044.  
<https://doi.org/10.1080/27684830.2022.2082044>.
- [8] T. Massarvva, Clinical outcomes of COVID-19 amongst HIV patients: a systematic literature review, *Epidemiol. Health*. 43 (2021), e2021036. <https://doi.org/10.4178/epih.e2021036>.
- [9] K.R. Cheneke, Optimal Control and Bifurcation Analysis of HIV Model, *Comput. Math. Methods Med*. 2023 (2023), 4754426. <https://doi.org/10.1155/2023/4754426>.
- [10] Z. Mukandavire, A.B. Gumel, W. Garira, et al. Mathematical analysis of a model for HIV-malaria co-infection, *Math. Biosci. Eng*. 6 (2009), 333-362. <https://doi.org/10.3934/mbe.2009.6.333>.
- [11] T.K. Ayele, E.F.D. Goufo, S. Mugisha, Mathematical modeling of HIV/AIDS with optimal control: A case study in Ethiopia, *Results Phys*. 26 (2021), 104263. <https://doi.org/10.1016/j.rinp.2021.104263>.

- [12] M.A. Hye, M.A.H.A. Biswas, M.F. Uddin, et al. Mathematical modeling of Covid-19 and dengue co-infection dynamics in bangladesh: optimal control and data-driven analysis, *Comput. Math. Model.* 33 (2022), 173-192. <https://doi.org/10.1007/s10598-023-09564-7>.
- [13] N.H. Shah, N. Sheoran, Y. Shah, Dynamics of HIV-TB co-infection model, *Axioms.* 9 (2020), 29. <https://doi.org/10.3390/axioms9010029>.
- [14] N.H. AlShamrani, A. Elaiw, A.A. Raezah, et al. Global dynamics of a diffusive within-host HTLV/HIV co-infection model with latency, *Mathematics.* 11 (2023), 1523. <https://doi.org/10.3390/math11061523>.
- [15] J. Ssebuliba, J.N. Nakakawa, A. Ssematimba, et al. Mathematical modelling of COVID-19 transmission dynamics in a partially comorbid community, *Part. Differ. Equ. Appl. Math.* 5 (2022), 100212. <https://doi.org/10.1016/j.padiff.2021.100212>.
- [16] A.M. Elaiw, A.D. Al Agha, S.A. Azoz, et al. Global analysis of within-host SARS-CoV-2/HIV coinfection model with latency, *Eur. Phys. J. Plus.* 137 (2022), 174. <https://doi.org/10.1140/epjp/s13360-022-02387-2>.
- [17] E. du Bruyn, C. Stek, R. Daroowala, et al. Effects of tuberculosis and/or HIV-1 infection on COVID-19 presentation and immune response in Africa, *Nat. Commun.* 14 (2023), 188. <https://doi.org/10.1038/s41467-022-35689-1>.
- [18] C. Danwang, J.J. Noubiap, A. Robert, et al. Outcomes of patients with HIV and COVID-19 co-infection: a systematic review and meta-analysis, *AIDS Res. Ther.* 19 (2022), 3. <https://doi.org/10.1186/s12981-021-00427-y>.
- [19] H.A. Gesesew, L. Mwanri, J.H. Stephens, et al. COVID/HIV co-infection: a syndemic perspective on what to ask and how to answer, *Front. Public Health.* 9 (2021), 623468. <https://doi.org/10.3389/fpubh.2021.623468>.
- [20] D. Basoulis, E. Mastrogianni, P.M. Voutsinas, et al. HIV and COVID-19 co-infection: epidemiology, clinical characteristics, and treatment, *Viruses.* 15 (2023), 577. <https://doi.org/10.3390/v15020577>.
- [21] J.L. Tamuzi, B.T. Ayele, C.S. Shumba, et al. Implications of COVID-19 in high burden countries for HIV/TB: A systematic review of evidence, *BMC Infect. Dis.* 20 (2020) 744. <https://doi.org/10.1186/s12879-020-05450-4>.
- [22] S.A. Azoz, A.M. Elaiw, E. Ramadan, et al. Global dynamics of a within-host COVID-19/AIDS coinfection model with distributed delays, *J. Math.* 2022 (2022), 9129187. <https://doi.org/10.1155/2022/9129187>.

- [23] S.W. Teklu, B.S. Kotola, A dynamical analysis and numerical simulation of COVID-19 and HIV/AIDS co-infection with intervention strategies, *J. Biol. Dyn.* 17 (2023), 2175920.  
<https://doi.org/10.1080/17513758.2023.2175920>.
- [24] C.A. Ouattara, A.G. Poda, Z.C. Méda, et al. Evaluation of the impact of COVID-19 in people coinfecting with HIV and/or tuberculosis in low-income countries: study protocol for mixed methods research in Burkina Faso, *BMC Infect. Dis.* 23 (2023), 108. <https://doi.org/10.1186/s12879-023-08076-4>.
- [25] B.S. Kotola, S.W. Teklu, Y.F. Abebaw, Bifurcation and optimal control analysis of HIV/AIDS and COVID-19 co-infection model with numerical simulation, *PLoS ONE.* 18 (2023), e0284759.  
<https://doi.org/10.1371/journal.pone.0284759>.
- [26] N. Ringa, M.L. Diagne, H. Rwezaura, et al. HIV and COVID-19 co-infection: A mathematical model and optimal control, *Inform. Med. Unlocked.* 31 (2022), 100978. <https://doi.org/10.1016/j.imu.2022.100978>.
- [27] P. van den Driessche, J. Watmough, Reproduction numbers and sub-threshold endemic equilibria for compartmental models of disease transmission, *Math. Biosci.* 180 (2002), 29-48. [https://doi.org/10.1016/s0025-5564\(02\)00108-6](https://doi.org/10.1016/s0025-5564(02)00108-6).
- [28] A. Fall, A. Iggidr, G. Sallet, J.J. Tewa, Epidemiological models and Lyapunov functions, *Math. Model. Nat. Phenom.* 2 (2007), 62-83. <https://doi.org/10.1051/mmnp:2008011>.
- [29] R.M. Neilan, S. Lenhart, An introduction to optimal control with an application in disease modeling, *DIMACS Ser. Discrete Math.* 75 (2010), 67-81.